Eur. Phys. J. D **3**, 229–236 (1998)

THE EUROPEAN PHYSICAL JOURNAL D

Monte-Carlo simulations of rotating clusters

F. Calvo[a] and P. Labastie

Laboratoire Collisions, Agrégats, Réactivité[b], IRSAMC, Université Paul Sabatier, 118, Route de Narbonne, 31062 Toulouse Cedex, France

Received: 27 January 1998 / Received in final form: 15 June 1998 / Accepted: 18 June 1998

Abstract. A new scheme for estimating densities of states at non zero angular momentum is proposed, using the Monte-Carlo (MC) and multiple histogram methods. It is based on a rigorous expression of the classical density of states for a rotating system. Two features appear: the centrifugal energy $\mathbf{L}\cdot\mathrm{I}^{-1}\mathbf{L}/2$ ($\mathbf{L}$ angular momentum and I the instantaneous inertia tensor in the center of mass reference frame) is added to the potential energy and the configurational densities of states is weighted by $1/\sqrt{\det \mathrm{I}}$. Comparing the MC results for the 13-atom Lennard-Jones cluster and a calculation based on molecular dynamics (MD) shows that this weight is important if the rotation induces a structural change at a finite temperature. The MC algorithm proves to be much more efficient than MD, even at finite $\mathbf{L}$.

PACS. 36.40.Ei Phase transitions in clusters – 82.30.Qt Isomerization and rearrangement – 05.20.Gg Classical ensemble theory

1 Introduction

Amongst the numerous theoretical studies of phases and phase changes in clusters in the past two decades, only a little deal of attention has been paid to the angular momentum problem. In most of the analytical or numerical works, its value was set to zero. This was a way to avoid the difficulties brought by extra inertial terms in the dynamics. However, real – experimental – conditions for isolated systems rarely produce nonrotating bodies. The semirigid approximation generally used in rovibrational spectroscopy may break down in the case of a rather floppy molecule and/or high angular momentum $\mathbf{L}$. Actually, the influence of rotation on the thermodynamical properties of finite atomic systems is presently poorly known.

A major advance in this topic occured with some results by Jellinek and Li (hereafter JL) [1–3]. They first separated the centrifugal terms in the energy of any isolated N-body system [1]. Their quenching method was applied to finding various isomers and stable (nonvibrating) equilibrium structures of rare gas clusters [2]. Further investigations on the vibrational dynamics of rotating clusters were also carried out by the same authors [3] along the lines of the work of Eckart [4]. More recently, Lohr and Huben [5] used the results of JL to derive exact expressions for the rotational energy dispersions in van der Waals clusters. The effect of rotation in cluster dynamics was investigated in evaporation studies [6–8], and the influence of a finite $\mathbf{L}$ on the chaotic dynamics was also considered [9].

The rigorous treatment of angular momentum conservation in statistical theories of molecular dissociation or reaction, included in phase space theory by Chesnavich and Bowers [10], benefited also from the work of JL [11]. Such theories require the accurate calculation of densities of states functions, which, in turn, can give microscopic rates [11] of evaporation [12,13] or fragmentation [14].

Densities of states are nevertheless primarily suited to the thermodynamical study at equilibrium, since they lead to all microcanonical *and* canonical properties [15]. Along with the numerous works of Berry [16–19], Wales [20–23] and coworkers, the Monte-Carlo (MC) multiple histogram method of Labastie and Whetten [15] has proven useful in the understanding of how melting occurs in finite systems. This method, precisely, extracts (microcanonical) densities of states functions from simulations, either MD or MC. Unfortunately, it does not include, at least in its current formulations [24–27], the angular momentum conservation, even with a zero value.

When an isolated cluster rotates, one cannot define the temperature by the mean value of the kinetic energy, because it includes the non-thermal rotation energy. JL [1] deduce instead the instantaneous temperature from the vibrational energy separated in the total energy. However, it is not clear whether the equipartition energy theorem can be applied *a priori*, especially when the cluster isomerizes spontaneously [2].

[a] e-mail: florent@yosemite.ups-tlse.fr
[b] UMR 5589, CNRS

In this article, we perform the full calculation of thermodynamical quantities of a cluster at fixed angular momentum $\mathbf{L}$. The methods used reconcile the multiple histogram method and a rigorous incorporation of the conservation of $\mathbf{L}$ in the microcanonical density of states. Here we make no assumption about the rigidity of the cluster. Besides the molecular dynamics histogram method proposed in reference [26], we here develop a new Monte-Carlo algorithm for extracting densities of states at constant $\mathbf{L}$. We test these methods on the melting of rotating 13-atom cluster bound by simple Lennard-Jones (LJ) potential. The results are presented and discussed in Section 3. Both MD and MC methods are found to agree, as in our previous work with no constraint on $\mathbf{L}$ [26]. We finally conclude and summarize in Section 4.

2 Methodology

In practice, isolated systems have constant total energy, but also constant total linear and angular momenta. Let us consider a classical N-body cluster bound by a potential energy function V depending only upon the cartesian coordinates vectors $\{\mathbf{r}_i\}$. If we denote by $\{\mathbf{p}_i\}$ the N momenta of the system and by $\{m_i\}$ the individual masses, the hamiltonian is $H(\{\mathbf{r}_i,\mathbf{p}_i\}) = \sum_i {\mathbf{p}_i}^2/2m_i + V(\{\mathbf{r}_j\})$. It is a constant of the motion, with a value equal to the total energy E. Taking into account the conservation of $\mathbf{P}$ and $\mathbf{L}$, the total linear and angular momenta respectively, the density of states Ω can be written as:

$$\Omega(E,\mathbf{P},\mathbf{L}) = \int \delta\left[H(\{\mathbf{r}_i,\mathbf{p}_i\}) - E\right] \times \delta\left[\sum_i \mathbf{p}_i - \mathbf{P}\right] \delta\left[\sum_i \mathbf{r}_i \times \mathbf{p}_i - \mathbf{L}\right] \times \prod_i d\mathbf{r}_i d\mathbf{p}_i. \quad (1)$$

Unless otherwise specified, products and sums over i range from $i = 1$ to $i = N$.

2.1 Full calculation of $\Omega(\mathbf{E},\mathbf{P},\mathbf{L})$

We propose in this paragraph an original way to calculate the density of states, equation (1). Other derivations have been given by Dumont [28], and independently by Smith [11].

We start by calling $\mathrm{P} = (\mathbf{p}_1,\ldots,\mathbf{p}_N)$ the $3N$-vector gathering all N individual linear momenta, and $\mathrm{R} = (\mathbf{r}_1,\ldots,\mathbf{r}_N)$. We note b the 6-vector $\mathrm{b} = (\mathbf{L},\mathbf{P})$, and a the real $a(\mathrm{R}) = E - V(\mathrm{R})$. We also define the $3N \times 3N$ diagonal tensor A such that ${\mathrm{P}}^T \mathrm{A} \mathrm{P} = \sum_i {\mathbf{p}_i}^2/2m_i$ (${\mathrm{P}}^T$ is the transpose of P):

$$\mathrm{A} = \begin{pmatrix} 1/2m_1 & & & & & \\ & 1/2m_1 & & & & \\ & & 1/2m_1 & & 0 & \\ & & & \ddots & & \\ & & & & & 1/2m_N \end{pmatrix}. \quad (2)$$

For all i, we define the antisymmetric 3×3 tensor J_i such that for any vector $\mathbf{u}$, we have $\mathrm{J}_i\mathbf{u} = \mathbf{u} \times \mathbf{r}_i$, that is

$$\mathrm{J}_i = \begin{pmatrix} 0 & z_i & -y_i \\ -z_i & 0 & x_i \\ y_i & -x_i & 0 \end{pmatrix} = \mathrm{J}_i(\mathrm{R}) \quad (3)$$

where $(x_i, y_i, z_i) = \mathbf{r}_i$ are the cartesian coordinates of atom i. By writing

$$\mathrm{B}(\mathrm{R}) = \begin{pmatrix} \mathrm{J}_1 & \mathbb{1} \\ \vdots & \vdots \\ \mathrm{J}_N & \mathbb{1} \end{pmatrix} \quad (4)$$

the $3N \times 6$ matrix with $\mathbb{1}$ the 3×3 identity tensor, we now have the following expression for the density of states

$$\Omega(E,\mathbf{P},\mathbf{L}) = \int d^{3N}\mathrm{R} \int d^{3N}\mathrm{P}\, \delta\left[{\mathrm{P}}^T \mathrm{A} \mathrm{P} - a\right] \delta\left[{\mathrm{B}}^T \mathrm{P} - \mathrm{b}\right] = \int d^{3N}\mathrm{R}\, \Lambda_{\mathrm{R}}(\mathrm{A},\mathrm{B},a,\mathrm{b}). \quad (5)$$

At a given configuration R, the integral over P is a function $\Lambda_{\mathrm{R}}(\mathrm{A},\mathrm{B},a,\mathrm{b})$, which can be exactly calculated (see Appendix A). The result is

$$\Lambda_{\mathrm{R}}(\mathrm{A},\mathrm{B},a,\mathrm{b}) = \frac{\pi^{s/2}}{\Gamma(s/2)} \times \frac{\left[a - {\mathrm{b}}^T ({\mathrm{B}}^T \mathrm{A}^{-1} \mathrm{B})^{-1} \mathrm{b}\right]^{s/2-1}}{\sqrt{\det \mathrm{A}}\sqrt{\det({\mathrm{B}}^T \mathrm{A}^{-1}\mathrm{B})}}. \quad (6)$$

where we have posed $s = 3N - 6$. Here we easily calculate

$${\mathrm{B}}^T \mathrm{A}^{-1} \mathrm{B} = 2 \begin{pmatrix} \mathrm{I} & -M\mathrm{J} \\ M\mathrm{J} & M\mathbb{1} \end{pmatrix} \quad (7)$$

where I is the 3×3 inertia matrix and J the 3×3 matrix such that $M\mathrm{J} = \sum_i m_i \mathrm{J}_i$. M is the total mass of the system, $M = \sum_i m_i$. Now we denote $\mathbf{r}_0 = (x_0, y_0, z_0)$ the c.o.m. coordinates of the cluster. In the reference frame with origin $\mathbf{r}_0$, the inertia tensor is I_0. I, I_0 and J are bound through the following relationship

$$\mathrm{I} = \mathrm{I}_0 - M\mathrm{J}^2. \quad (8)$$

It can also be shown that $\det({\mathrm{B}}^T \mathrm{A}^{-1}\mathrm{B}) = 2^6 M^3 \det \mathrm{I}_0$. The matrix ${\mathrm{B}}^T \mathrm{A}^{-1}\mathrm{B}$ can be inverted as

$$({\mathrm{B}}^T \mathrm{A}^{-1}\mathrm{B})^{-1} = \frac{1}{2} \begin{pmatrix} \mathrm{I}_0^{-1} & \mathrm{I}_0^{-1}\mathrm{J} \\ -\mathrm{J}\mathrm{I}_0^{-1} & \mathbb{1}/M - \mathrm{J}\mathrm{I}_0^{-1}\mathrm{J} \end{pmatrix}, \quad (9)$$

and, by denoting $\mathbf{L}_0 = -\mathrm{J}\mathbf{P} = \mathbf{r}_0 \times \mathbf{P}$ the translational angular momentum of the system, we have

$${\mathrm{b}}^T ({\mathrm{B}}^T \mathrm{A}^{-1}\mathrm{B})^{-1} \mathrm{b} = (\mathbf{L} - \mathbf{L}_0)^T \frac{\mathrm{I}_0^{-1}}{2} (\mathbf{L} - \mathbf{L}_0) + \frac{\mathbf{P}^2}{2M}. \quad (10)$$

Finally, the result can be written in complete generality:

$$\Omega(E,\mathbf{P},\mathbf{L}) = \frac{(2\pi)^{s/2}}{\Gamma(s/2)}\frac{\prod_i m_i^{3/2}}{M^{3/2}} \times \int \frac{d^{3N}\mathrm{R}}{\sqrt{\det \mathrm{I}_0}} \left[E - V(\mathrm{R}) - \mathbf{P}^2/2M - (\mathbf{L}-\mathbf{L}_0)^{T}\frac{\mathrm{I}_0^{-1}}{2}(\mathbf{L}-\mathbf{L}_0)\right]^{s/2-1}. \quad (11)$$

From now on, we restrict our study to the c.o.m. reference frame. This does not affect the thermodynamics. In this frame $\mathbf{P} = \mathbf{0}$ and $\mathbf{L}_0 = \mathbf{0}$. $\mathbf{L}$ is now the internal angular momentum. The reason why $\mathbf{P}$ disappears from the equation while $\mathbf{L}$ does not is because it is impossible to define "the" reference frame where the molecule does not rotate. However, the total density of states may still be factorized as a convolution product of the kinetic (Ω_{K}) and configurational (Ω_{C}) densities of states:

$$\Omega(E,\mathbf{P}=\mathbf{0},\mathbf{L}) = \Omega(E,\mathbf{L}) = \int_0^E \Omega_{K}(K)\Omega_{C}(E-K,\mathbf{L})dK \quad (12)$$

where $\Omega_{K}(E) \propto E^{(3N-8)/2}$ and, with, from now on $\mathrm{I}_0 = \mathrm{I}$:

$$\Omega_{C}(E_{C},\mathbf{L}) \propto \int \delta\left[E_{C} - V_{\mathbf{L}}(\mathrm{R})\right]\frac{d^{3N}\mathrm{R}}{\sqrt{\det \mathrm{I}}}\cdot \quad (13)$$

In the latter equation, $V_{\mathbf{L}}(\mathrm{R})$ is the rovibrational potential energy previously separated from the total energy by JL [1]:

$$V_{\mathbf{L}}(\mathrm{R}) = V(\mathrm{R}) + \mathbf{L}^{T}\frac{\mathrm{I}^{-1}}{2}\mathbf{L}. \quad (14)$$

This effective potential-energy surface has been extensively studied, in its topographic details (stationary points), by Miller and Wales [7]. The main result of this paragraph is that the thermodynamics of the cluster is not only governed by the rovibrational potential function, but a geometrical factor is now included into the configurational density of states. This is also the case when the cluster does not rotate, since this weight is independent of $\mathbf{L}$. This factor $1/\sqrt{\det \mathrm{I}}$, which reduces to $1/I$ in the case of linear molecules, was previously found in terms of the principal momenta of inertia by several authors [11,28–30] who used and applied it to the case of simple molecular systems.

2.2 Extracting densities of states from simulations

The calculation of thermodynamical properties from the computation of densities of states may be carried out with the multiple histogram method of Labastie and Whetten [15]. First developed in statistical physics [31], it has been since largely used in the cluster community, mainly in the study of isomerization and phase changes [15,24–27,32–35] and also in evaporation studies [12,13]. Its original formulation was based on canonical simulations at fixed temperature T. We extended in a previous work the algorithm to isoergic microcanonical simulations [26]. We now further extend it to include the angular momentum constraint in isolated systems, in both Gibbs ensembles. We first consider the microcanonical case.

2.2.1 Microcanonical ensemble

At fixed number of atoms N, total energy E and angular momentum $\mathbf{L}$, the probability density for the system having a configurational rovibrational energy $V_{\mathbf{L}}$ is given by

$$P_{\mathbf{L}}(E,V_{\mathbf{L}}) = \Omega_{C}(V_{\mathbf{L}},\mathbf{L})\Omega_{K}(E-V_{\mathbf{L}})/\Omega(E,\mathbf{L}) \quad (15)$$

with the normalization $\int_0^E P_{\mathbf{L}}(E,V_{\mathbf{L}})dV_{\mathbf{L}} = 1$. We perform several MD simulations at different total energies $\{E_i\}$ and at constant $\mathbf{L}$. We then bin together the values of $V_{\mathbf{L}}$ by counting the number of times a value $V_{\mathbf{L}}^j \pm \Delta V$ occurs. This number is normalized to a probability p_{ij} of occurrence of the value $V_{\mathbf{L}}^j$ at a given total energy E_i. According to equation (15), we have

$$p_{ij} = \alpha_i \Omega_j (E_i - V_{\mathbf{L}}^j)^{s/2-1} \quad (16)$$

where $\Omega_j = \Omega_{C}(V_{\mathbf{L}}^j,\mathbf{L})$, $\alpha_i = 1/\Omega(E_i,\mathbf{L})$. However the p_{ij} are obtained with a statistical error. We have to resort to a least-squares minimization to estimate the $\{\alpha_i\}$ and $\{\Omega_j\}$ [24,26]. We thus obtain the function $\Omega_{C}(V_{\mathbf{L}},\mathbf{L})$ over a wide range of values of $V_{\mathbf{L}}$ and, from equation (15), the probability of occurence of the kinetic energy K at a given total energy. The microcanonical temperature is then [36]:

$$k_{B}T_{\mathbf{L}}(E) = \left(\frac{s-2}{2}\langle K_{\mathbf{L}}^{-1}\rangle\right)^{-1} \quad (17)$$

where $\langle K_{\mathbf{L}}^{-1}\rangle$ is the microcanonical average of the vibrational instantaneous kinetic energy $K_{\mathbf{L}}$.

The present treatment is just a rewriting of reference [26] with the rovibrational potential energy $V_{\mathbf{L}}$ replacing V. In the simulations, one needs to compute at each time step the inertia tensor and the energy of overall rotation of the "rigid body" associated with same R and $\mathbf{L}$, that is [1] $\mathbf{L}^{T}\mathrm{I}^{-1}\mathbf{L}/2$. Since MD naturally conserves $\mathbf{L}$, the geometrical weight $1/\sqrt{\det \mathrm{I}}$ is automatically included in the probability distributions recorded.

2.2.2 Canonical ensemble

In the canonical ensemble at temperature T, the fundamental quantity of interest is the partition function $Q(T,\mathbf{P},\mathbf{L})$:

$$Q(T,\mathbf{P},\mathbf{L}) = \int \delta\left[\sum_i \mathbf{p}_i - \mathbf{P}\right]\delta\left[\sum_i \mathbf{r}_i\times\mathbf{p}_i - \mathbf{L}\right] \times \exp\left[-\beta H(\{\mathbf{r}_i,\mathbf{p}_i\})\right]\prod_i d\mathbf{r}_i d\mathbf{p}_i \quad (18)$$

where $\beta = 1/k_B T$. This quantity may be calculated by a Laplace transform of the density of states, equation (11), to finally obtain

$$Q(T,\mathbf{P},\mathbf{L}) = \frac{(2\pi)^{s/2}}{\beta^{s/2}} \frac{\prod_i m_i^{3/2}}{M^{3/2}} \exp\left[-\beta \frac{\mathbf{P}^2}{2M}\right] \times \int \frac{d^{3N}\mathrm{R}}{\sqrt{\det \mathrm{I}_0}} \exp\left[-\beta \left(V(\mathrm{R}) + (\mathbf{L}-\mathbf{L}_0)^T \frac{\mathrm{I}_0^{-1}}{2} (\mathbf{L}-\mathbf{L}_0)\right)\right]. \quad (19)$$

Q factorizes as a product of a kinetic term $Q_K(T,\mathbf{P},\mathbf{L})$ and a configurational term $Q_C(T,\mathbf{P},\mathbf{L})$, with

$$Q_K(T,\mathbf{P},\mathbf{L}) = \frac{(2\pi)^{s/2}}{\beta^{s/2}} \frac{\prod_i m_i^{3/2}}{M^{3/2}} \exp\left[-\beta \frac{\mathbf{P}^2}{2M}\right]. \quad (20)$$

In the c.o.m. reference frame, the configuration integral $Q_C(T,\mathbf{P}=\mathbf{0},\mathbf{L})$ is given by

$$Q_C(T,\mathbf{L}) = \int \frac{\exp\left[-\beta V_{\mathbf{L}}(\mathrm{R})\right]}{\sqrt{\det \mathrm{I}}} d^{3N}\mathrm{R}. \quad (21)$$

The Boltzmann probability to observe the rovibrational energy $V_{\mathbf{L}}$ corresponding to the configuration R is given in the canonical ensemble by

$$P_{\mathbf{L}}(T, V_{\mathbf{L}}(\mathrm{R})) = \Omega_C(V_{\mathbf{L}},\mathbf{L}) \frac{\exp -\beta V_{\mathbf{L}}}{\sqrt{\det \mathrm{I}(\mathrm{R})}} / Q_C(T,\mathbf{L}). \quad (22)$$

To obtain such distributions, Monte-Carlo simulations, and more generally canonical simulations, may incorporate the weight $1/\sqrt{\det \mathrm{I}}$ into their sampling algorithm. We propose to bias the Markov chain in the following way:

$$\frac{p(a \to b)}{p(b \to a)} = \sqrt{\frac{\det \mathrm{I}_a}{\det \mathrm{I}_b}} \exp\left[-\beta (V^b_{\mathbf{L}} - V^a_{\mathbf{L}})\right]. \quad (23)$$

Here, a and b are two different points in the Markov chain, that is two different geometries of the system. $p(a \to b)$ is the probability of accepting the jump from configuration a toward configuration b, and $V^a_{\mathbf{L}}$ is the rovibrational energy of configuration a. Therefore, MC simulations must be carried out on the $V_{\mathbf{L}}$ surface, with a non-boltzmannian weight $1/\sqrt{\det \mathrm{I}}$. This again requires the calculation of the inertia tensor I at each MC step, for computing both $V_{\mathbf{L}}$ and the geometrical weight. Such simulations will be denoted as "weighted Monte-Carlo" (WMC), in contrast to non weighted simulations performed on the $V_{\mathbf{L}}$ surface but with no geometrical weight, hereafter refered to as to "unweighted Monte-Carlo" (UMC).

To estimate the configurational density of states from equation (22) and the multiple histogram method, we perform several simulations at different temperatures $\{T_i\}$, according to equation (23) and at fixed vector $\mathbf{L}$. The probability for observing the rovibrational energy $V_{\mathbf{L}}$ is given by

$$p_{ij} = \alpha_i \Omega_j \exp(-\beta_i V^j_{\mathbf{L}}) \quad (24)$$

where $\Omega_j = \Omega_C(V^j_{\mathbf{L}},\mathbf{L})$, $\alpha_i = 1/Q_C(T_i,\mathbf{L})$. Here again, a least-squares fit on the $\{p_{ij}\}$ gives the Ω_j's.

Unweighted MC simulations can also be used, provided that the quantity $1/\sqrt{\det \mathrm{I}}$ has been evaluated and recorded at each energy $V_{\mathbf{L}}$. The histogram method applies in the same way as above, by scaling the p_{ij} directly calculated from the simulation by the corresponding weights.

We now illustrate the methods developed in this section on the calculation of the calorific curves of the 13-atom Lennard-Jones cluster.

3 Results and discussion

The classical 12–6 LJ potential is generally used to model the interaction between atoms in rare gas clusters:

$$V(\mathrm{R}) = \sum_{i<j} 4\varepsilon \left[\left(\frac{\sigma}{r_{ij}}\right)^{12} - \left(\frac{\sigma}{r_{ij}}\right)^{6}\right]. \quad (25)$$

To this pair potential, we add a hard-wall repulsive sphere $V_{rep}(R)$ which was previously used by Wales [22]:

$$V_{rep}(r_i) = \begin{cases} 4\varepsilon \left[\left(\frac{\sigma}{R_0 - r_i}\right)^{12} - \left(\frac{\sigma}{R_0 - r_i}\right)^{6}\right] + \varepsilon, & R_0 - r_i < 2^{1/6}\sigma; \\ 0, & R_0 - r_i \geq 2^{1/6}\sigma. \end{cases} \quad (26)$$

R_0 is the radius of the container, whose center is constantly fixed to the cluster c.o.m., which is itself located at the origin of the reference frame. In the following, LJ units ($\varepsilon = \sigma = m = 1$) are used throughout. The size of the container is taken as $R_0 = 3.5$ for all angular momenta. Confining the cluster has little influence over a wide range of temperatures, because the radius of the 13-atom LJ-cluster at rest is about 1.5 LJ units. Without confinement however, the cluster would begin to evaporate at a temperature close to the solid-liquid transition. The main effect of the container is to prevent this evaporation in a wider range of temperature, including the whole transition region. The calorific curves that we show below are drawn up to the point where evaporation becomes predominent.

MD simulations are carried out with the velocity version of the Verlet algorithm [37]. This algorithm keeps the total energy and angular momentum constant to better than 1 in 10^5 parts for simulations of 10^6 time steps. The first 3×10^5 steps are not recorded in order to thermalize the cluster.

We perform MC simulations with the standard Metropolis method, biased according to equation (23). Each step of the Markov chain consists in a random move of all the atoms, the c.o.m. being kept fixed. At each temperature, MC simulations also run for 10^6 steps, whose first 3×10^5 are discarded to allow thermalization.

In both cases, the equilibrium structure has to be known as a starting point at low temperature. They were

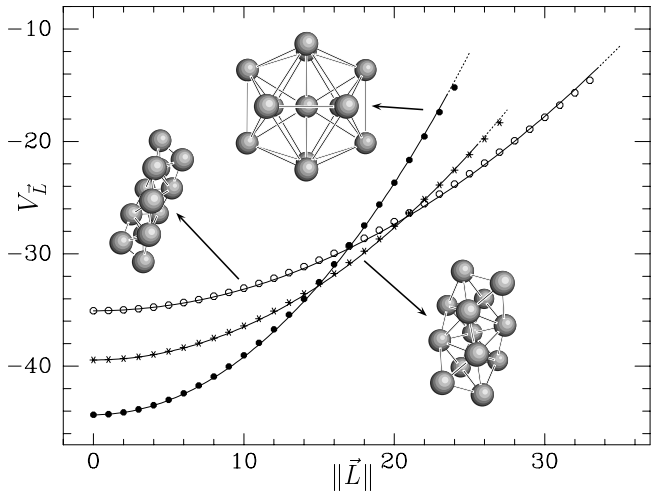

Fig. 1. Equilibrium geometries and energies as a function of $\|\mathbf{L}\|$, for rotation around the C_2 axis. The dotted lines denote unstable structures which spontaneously isomerize or split up.

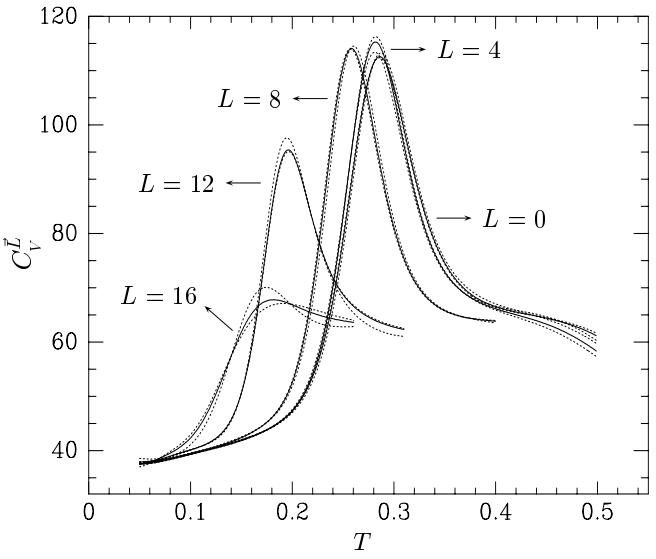

Fig. 2. Heat capacity $C_V^{\mathbf{L}}$ *versus* the canonical temperature T for slowly rotating LJ_{13}. The ground state of the cluster is icosahedral D_{2h}, and the angular momentum is in the range $0 \leq L \leq 16$ LJ units. The solid lines are the results of MD simulations analysed by the multiple histogram method, the dashed lines are two results of MC simulations weighted by the geometrical factor $1/\sqrt{\det \mathrm{I}}$. $C_V^{\mathbf{L}}$ is given in units of k_B.

obtained by quenching methods [1,7,8], for different values of $\mathbf{L}$, starting from $\mathbf{0}$ up to fragmentation. Several orientations (C_2, C_3 and C_5) of the rotation axis were investigated, but the thermodynamical results were found to be independent on this choice, which is consistent with the expected isotropy of statistical thermodynamics [38]. Besides standard quenching methods, a global optimization scheme such as Monte-Carlo simulated annealing can also be used. However, in order to obtain the same results with a MC algorithm and a dynamical method, we have to constrain the symmetry axis [2]. This requires that elementary displacements $\{\delta\mathbf{r}_i\}$ around the current positions $\{\mathbf{r}_i\}$ verify the Eckart-type condition [4]

$$\sum_i m_i \mathbf{r}_i \times \delta\mathbf{r}_i = \mathbf{0} \tag{27}$$

at each MC step. We shall refer to this technique in the following as "constrained Monte-Carlo" (CMC).

The energies and geometries of the ground states are diplayed in Figure 1 as a function of the magnitude of $\mathbf{L}$, for rotation around the C_2 axis. We find three different structures, which becomes less and less spherical as $\|\mathbf{L}\|$ increases. At low $\mathbf{L}$, the ground structure is nearly icosahedral with symmetry D_{2h} [2]. When $\mathbf{L}$ reaches about 15 LJ units, this D_{2h} geometry becomes less stable than a C_2 structure with larger I (hence a slower rotating motion.) This latter structure remains the ground one up to about $L \simeq 21$ LJ units. At last, an other isomer, even less spherical, but also with symmetry C_2, is the most stable geometry until the angular momentum is too high and the cluster spontaneously splits up [2]. This occurs at $L = L_{max} \simeq 32$ LJ units. The energies of all these isomers roughly grow with $\mathbf{L}$ as $V(\mathbf{L}) \simeq V(0) + L^2/2I_0$, where I_0 is the momentum of inertia at $\mathbf{L} = \mathbf{0}$.

The thermodynamical results in the range $0 \leq \|\mathbf{L}\| \leq 16$ LJ units are given in Figure 2. We plotted the canonical heat capacity *versus* temperature T. These curves were calculated with the densities of states extracted with the multi-histogram method from either MD or MC simulations. They show three different portions [15,22,32]. At low temperature, C_V is roughly constant and close to the value of harmonic approximation, $C_V^{HA} = (3N-6)k_B$. The cluster is in its rigidlike state similar in many respects to the bulk solid phase, and only vibrates around its ground structure. At the other end, the high temperature region, the cluster is entirely fluid and C_V is larger than in the solid phase by about 50%, but still approximately constant. Between these two regions, a high peak marks the occurence of a first order phase transition rounded by finite size effects. The top of the C_V peak can be used to define the melting point. As the magnitude of $\mathbf{L}$ increases, the melting temperature decreases and the C_V peak becomes wider. At low angular momentum, $\|\mathbf{L}\| \lesssim 8$ LJ units, the total energy at melting is roughly constant. Since this energy is $V_{ground}(\mathbf{L}) + (3N-6)k_B T_m$ and $V_{ground}(\mathbf{L}) \simeq V_{ground}(\mathbf{0}) + L^2/2I_0$, we have $T_m(L) \simeq T_m(0) - L^2/[(3N-6)k_B I_0]$, which is the observed behavior.

At higher magnitude of $\mathbf{L}$, the stability of the cluster is expected to decrease [2,8]. This is a reason for the steady decrease of the transition temperature T_m. Actually, it is more and more difficult to prevent evaporation of the cluster, which is a reason for the almost complete disappearance of the transition peak in Figure 2.

Figure 2 shows clearly a very good agreement between the MD and MC results: both algorithms, along with the subsequent histogram analysis, produce the same

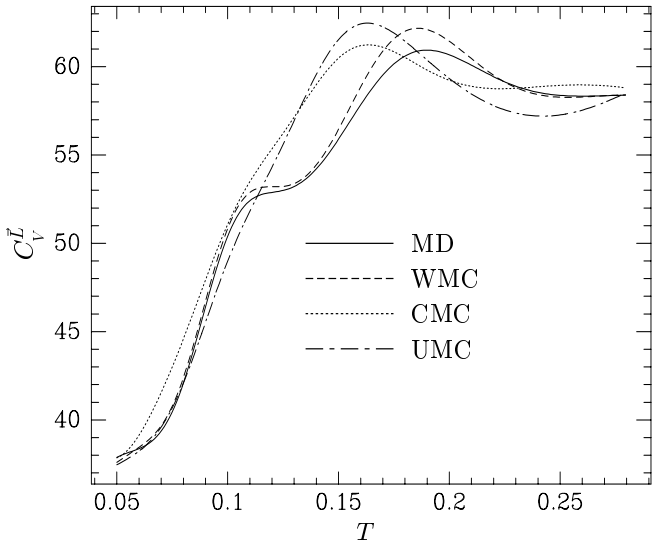

Fig. 3. Heat capacity $C_V^{\mathbf{L}}$ *versus* T for LJ_{13} spinning at $L = 18$ LJ units. The ground state is ellipsoidal with symmetry C_2. Four curves are presented, which correspond to MD, WMC, UMC and CMC simulations (see text). $C_V^{\mathbf{L}}$ is given in units of k_B.

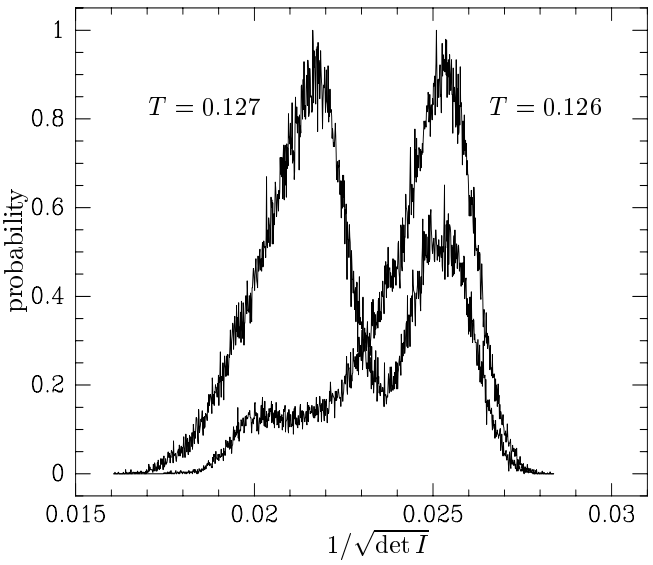

Fig. 4. Probability distribution of the geometrical weight $1/\sqrt{\det \mathrm{I}}$ in weighted Monte-Carlo simulations near the preliminary hump of the heat capacity. The probabilities are not normalized.

calorific curves within statistical errors. However other MC calorific curves computed without the geometrical weight (CMC and UMC with no weighting in the histograms), not plotted in Figure 2, *also produce similar results*. The inclusion of the $1/\sqrt{\det \mathrm{I}}$ weight seems thus of an academic character rather than of any use. We show now a case where this factor is more important.

The heat capacity for $\|\mathbf{L}\| = 18$ LJ units is presented in Figure 3. The ground state has a nearly ellipsoidal shape with symmetry C_2. We plotted in Figure 3 the results of MD simulations, unweighted MC, constrained MC and weighted MC simulations. Again, we find a good agreement between MD and WMC curves. But now, the agreement between MD and both UMC and CMC curves is rather poor. In particular, the results of MD and WMC exhibit a preliminary hump near $T \sim 0.12$ LJ units, whereas the top of the C_V bump occurs near $T \sim 0.18$. UMC and CMC curves roughly appear as averages of these two events, with a melting temperature located at about $T \sim 0.16$. When the weight is taken into account in the histogram method from UMC simulations, we find results similar to those obtained by weighting the acceptance probability (WMC).

To understand the first hump in the heat capacity, we calculated the probability distribution of the weight $1/\sqrt{\det \mathrm{I}}$ at several temperatures near $T \sim 0.12$. The results, from WMC, are given in Figure 4. They show a very clear bimodality near the transition temperature 0.127. It can be easily seen (for instance by regular quenches) that the low values reached by the weight $1/\sqrt{\det \mathrm{I}}$ are associated with highly nonspherical structures. In MD simulations, these structures have a much lower rotation velocity, hence a higher stability. UMC and CMC algorithms do not take this dynamical stabilization into account, and miss the structural transition preliminar to melting on the caloric curve. It is rather remarkable that a MC algorithm, which is static by nature can incorporate dynamical effects. Owing to the gain in time of the MC method, it seems that even for rotating species, MC is preferable to MD, provided that a careful inclusion of the weight factor is done, either in the Markov chain itself or in the weighting of the histograms.

4 Conclusion

In the present work, we have developed a Monte-Carlo method for calculating exact densities of states when a constraint on the angular momentum is imposed. This new method has been used to compute the (canonical) thermodynamical properties of the LJ_{13} cluster with the multiple histogram method and compare them to the same curves calculated from molecular dynamics results.

Our new MC scheme was carried out with a Metropolis sampling on the rovibrational potential energy surface, weighted by $1/\sqrt{\det \mathrm{I}}$ where I is the local inertia tensor. The results obtained with this algorithm are in very good agreement with MD results. Actually, at low $\mathbf{L}$, the weighting is not necessary and conventional (*i.e.* nonweighted) Monte-Carlo gives also the same results as MD. In particular, a simple non-weighted MC method on the pure LJ potential is equivalent to simulating a non-rotating cluster. However, without the inclusion of the weight, there are some situations where it is impossible to obtain an

agreement between MD and MC methods. The calculation of the weight, at each MC step, does not involve any extra computing since it is already required for the rovibrational energy term. Therefore, as in our previous study on nonrotating clusters [26], the MC method at $L \neq 0$ is again much cheaper (and easier) to implement than the MD method for the same statistical results. In our opinion, this makes Monte-Carlo methods the best choice for studying the equilibrium thermodynamics of rotating (and nonrotating) clusters. Furthermore, as far as canonical Nosé-Hoover-like molecular dynamics does not allow angular momentum conservation (except at $L = 0$ [12]), MC seems a more straightforward and natural method for investigating the behavior of a rotating cluster at constant temperature. In turn, such MC methods can be used to calculate free-energy differences of rotating systems along a classical reaction coordinate [39].

The specific cluster studied here shows an interesting behavior. At low magnitude of the angular momentum **L**, the transition temperature between the solidlike and liquidlike phases decreases with **L**, together with the mechanical stability, linearly as L^2. Up to about $L \sim 16$ LJ units, the centrifugal effects only smooth the transition while the ability for fragmentation rises. When L reaches 18 LJ units, a preliminary structural transition occurs between the C_2 ground state and even more nonspherical geometries which tend to lower the rotation velocity. The heat capacity exhibits a small bump at $T = 0.13$ which reflects this structural transition.

With the help of the multiple histogram method, we have calculated accurate anharmonic densities of states at constant angular momentum. Such functions fully characterize the microcanonical properties of an isolated atomic or molecular system. Statistical models such as phase space theory use exact densities of states to predict evaporation [12,13] or dissociation [14] rates. Coupled with a method such as adiabatic switching [40] which allows to determine absolute values, the histogram technique developed in this work should allow the complete calculation of similar rates at $\mathbf{L} \neq \mathbf{0}$, hence a better understanding of evaporation and fragmentation processes in clusters, among other processes and phenomena.

Support by the CNRS, the Région Midi-Pyrénées, the Université Paul Sabatier and the MESR is gratefully acknowledged.

Appendix

The density of states of any classical N-body system is given in equation (5). Its evaluation requires to calculate

$$\Lambda(\mathrm{A},\mathrm{B},a,\mathrm{b}) = \int d^m\mathrm{P}\,\delta\Big[\mathrm{P}^{T}\mathrm{A}\mathrm{P}-a\Big]\,\delta\Big[\mathrm{B}^{T}\mathrm{P}-\mathrm{b}\Big] \quad \text{(A.1)}$$

at each geometry R. In equation (A.1), A is a $m \times m$ symmetric positive definite matrix, a is a real scalar, B a $m \times n$ matrix and b a n-vector. a, B and B depend on the R which is kept constant in the integration. Here $m = 3N$ and $n = 6$, but we only need $m \geq n$. The integration on P is performed on the whole m-space, denoted $\mathcal{E}$.

Let us define a new basis U in $\mathcal{E}$. First, the equation $\mathrm{B}^{T}\mathrm{P} = \mathrm{O}$ defines a vector space $\mathcal{E}_1$ of dimension $m-n$. Since A is a symmetric positive definite matrix, it can be used to define a scalar product in $\mathcal{E}$. We define $\mathcal{E}_2$ as the orthogonal supplement of $\mathcal{E}_1$ respective to this scalar product: $\mathcal{E} = \mathcal{E}_1 \oplus \mathcal{E}_2$. U is now chosen as an othonormal basis respective to the same scalar product, with the first $m-n$ vectors in $\mathcal{E}_1$ and the last n in $\mathcal{E}_2$. It has the following properties

$$\mathrm{U}^{T}\mathrm{A}\mathrm{U} = \mathbb{1}; \quad \text{(A.2)}$$

$$\mathrm{B}^{T}\mathrm{U} = (\,\mathrm{O}\,|\,\mathrm{V}\,); \quad \text{(A.3)}$$

where V is a $n \times n$ matrix. In the new basis, the vector P becomes $\mathrm{x} = \mathrm{U}^{\mathrm{T}}\mathrm{P} = (\mathrm{x}_1, \mathrm{x}_2)$ with $\mathrm{x}_1 \in \mathcal{E}_1$ and $\mathrm{x}_2 \in \mathcal{E}_2$, and Λ becomes

$$\Lambda = \int d^{m-n}\mathrm{x}_1 d^n\mathrm{x}_2\,\delta\Big[\mathrm{x}_1^{T}\mathrm{x}_1 + \mathrm{x}_2^{T}\mathrm{x}_2 - a\Big]\,\delta[\mathrm{V}\mathrm{x}_2 - \mathrm{b}]\,|\det \mathrm{U}|. \quad \text{(A.4)}$$

From equation (A.2) we have $\mathrm{V}\mathrm{V}^{T} = \mathrm{B}^{T}\mathrm{A}^{-1}\mathrm{B}$, hence $|\det \mathrm{V}|^2 = \det(\mathrm{B}^{T}\mathrm{A}^{-1}\mathrm{B})$. Let us assume that $\mathrm{B}^{T}\mathrm{A}^{-1}\mathrm{B}$ is invertible (this can be easily checked in our case.) So is V, which allows to change variable from x_2 to $\mathrm{x}_3 = \mathrm{V}\mathrm{x}_2$. Then we have

$$\Lambda = \int d^{m-n}\mathrm{x}_1 d^n\mathrm{x}_3\,\delta\Big[\mathrm{x}_1^{T}\mathrm{x}_1 + \mathrm{x}_3^{T}(\mathrm{V}\mathrm{V}^{T})^{-1}\mathrm{x}_3 - a\Big] \times\delta[\mathrm{x}_3 - \mathrm{b}]\,\frac{|\det \mathrm{U}|}{|\det \mathrm{V}|}. \quad \text{(A.5)}$$

The integration on x_3 can be performed, it leads to

$$\Lambda = \int d^{m-n}\mathrm{x}_1\,\delta\Big[\mathrm{x}_1^{T}\mathrm{x}_1 - \alpha\Big]\,\frac{|\det \mathrm{U}|}{|\det \mathrm{V}|}, \quad \text{(A.6)}$$

where $\alpha = a - \mathrm{b}^{T}(\mathrm{V}\mathrm{V}^{T})^{-1}\mathrm{b}$. Now we define a new variable $\mathrm{z} = \sqrt{\alpha}\mathrm{x}_1$:

$$\Lambda = \alpha^{(m-n-2)/2}\int d^{m-n}\mathrm{z}\,\delta[\mathrm{z}^{T}\mathrm{z} - 1]\,\frac{|\det \mathrm{U}|}{|\det \mathrm{V}|}\,. \quad \text{(A.7)}$$

Since $|\det \mathrm{U}| = 1/\sqrt{\det \mathrm{A}}$ from equation (A.2), Λ can be expressed as

$$\Lambda = \frac{\alpha^{(m-n-2)/2}}{\sqrt{\det \mathrm{A}}\sqrt{\det(\mathrm{B}^{T}\mathrm{A}^{-1}\mathrm{B})}}\mathcal{S}(m-n). \quad \text{(A.8)}$$

In this equation, $\mathcal{S}(p)$ is the surface of the hypersphere of dimension p: $\mathcal{S}(p) = \pi^{p/2}/\Gamma(p/2)$. At last we obtain

$$\Lambda(\mathrm{A},\mathrm{B},a,\mathrm{b}) = \frac{\pi^{(m-n)/2}}{\Gamma((m-n)/2)} \times \frac{[a - \mathrm{b}^{T}(\mathrm{B}^{T}\mathrm{A}^{-1}\mathrm{B})^{-1}\mathrm{b}]^{(m-n-2)/2}}{\sqrt{\det \mathrm{A}}\sqrt{\det(\mathrm{B}^{T}\mathrm{A}^{-1}\mathrm{B})}}\,. \quad \text{(A.9)}$$

References

1. J. Jellinek, D. H. Li, Phys. Rev. Lett. **62**, 241 (1989).
2. D.H. Li, J. Jellinek, Z. Phys. D **12**, 177 (1989).
3. J. Jellinek, D.H. Li, Chem. Phys. Lett. **169**, 380 (1990).
4. C. Eckart, Phys. Rev. **47**, 552 (1935).
5. L.L. Lohr, C.H. Huben, J. Chem. Phys. **99**, 6369 (1993).
6. A.J. Stace, J. Chem. Phys. **93**, 6502 (1991).
7. M.A. Miller, D.J. Wales, Mol. Phys. **89**, 533 (1996).
8. F. Calvo, F. Spiegelmann, Z. Phys. D **41**, 195 (1997).
9. Y. Yurtsever, Europhys. Lett. **37**, 91 (1997).
10. W.J. Chesnavich, M.T. Bowers, J. Chem. Phys. **66**, 2306 (1977).
11. S.C. Smith, J. Chem. Phys. **97**, 2406 (1992).
12. S. Weerasinghe, F.G. Amar, J. Chem. Phys. **98**, 4967 (1993).
13. P. Parneix (private communication).
14. M.J. López, J. Jellinek, Phys. Rev. A **50**, 1445 (1994).
15. P. Labastie, R.L. Whetten, Phys. Rev. Lett. **65**, 1567 (1990).
16. R.S. Berry, J. Jellinek, G. Natanson, Chem. Phys. Lett. **107**, 227 (1984).
17. R.S. Berry, D.J. Wales, J. Chem. Phys. **92**, 4473 (1990).
18. R.E. Kunz, R.S. Berry, Phys. Rev. E **49**, 1895 1994.
19. J.P. Rose, R.S. Berry, J. Chem. Phys. **98**, 3246 (1993).
20. D.J. Wales, R.S. Berry, Phys. Rev. Lett. **73**, 2875 (1994).
21. D.J. Wales, J. Chem. Phys. **101**, 3750 (1994).
22. D.J. Wales, Mol. Phys. **78**, 151 (1993).
23. R.M. Lynden-Bell, D.J. Wales, J. Chem. Phys. **101**, 1460 (1994).
24. R. Poteau, F. Spiegelmann, P. Labastie, Z. Phys. D **30**, 57 (1994).
25. H.-P. Cheng, Z. Li, R.L. Whetten, R.S. Berry, Phys. Rev. A **46**, 791 (1992).
26. F. Calvo, P. Labastie, Chem. Phys. Lett. **247**, 395 (1995).
27. G.S. Fanourgakis, S.C. Farantos, P. Parneix, P. Bréchignac, J. Chem. Phys. **106**, 4954 (1997).
28. R.S. Dumont, J. Chem. Phys. **95**, 9172 (1991).
29. G. Nyman, S. Nordholm, H.W. Schranz, J. Chem. Phys. **93**, 6767 (1990).
30. S.C. Smith, J. Chem. Phys. **95**, 3404 (1991).
31. A.M. Ferrenberg, R.H. Swendsen, Phys. Rev. Lett. **63**, 1195 (1989); C. Bichara, J.-P. Gaspard, J.-C. Mathieu, Phys. Lett. A **119**, 462 (1987).
32. C.J. Tsai, K.D. Jordan, J. Chem. Phys. **99**, 6957 (1993).
33. F. Calvo, P. Labastie, J. Phys. Chem. B **102**, 2051 (1998).
34. F. Calvo, F. Spiegelmann, Phys. Rev. B **54**, 10949 (1996).
35. F. Calvo, P. Labastie, Chem. Phys. Lett. **248**, 233 (1996).
36. E.M. Pearson, T. Halicioglu, W.A. Tiller, Phys. Rev. A **32**, 3030 (1985).
37. M.P. Allen, D.J. Tildesley, *Computer Simulations of Liquids* (Oxford, 1987).
38. L. Landau, E. Lifchitz, *Statistical Physics* (Mir, 1967).
39. F. Calvo, Chem. Phys. Lett. **291**, 393 (1998).
40. W.P. Reinhardt, J. Mol. Struct. **223**, 157 (1990).